RESEARCH ARTICLE

Seasonal variations in water quality and phytoplankton–bacteria interactions mediated through dissolved organic matter in New Jersey coastal waters

Shuting Liu[1] · Chelsea Oti[1] · Benjamin Aharoni[2] · Derek J. Melendez[1] · Spencer Thompson[1]

Abstract

New Jersey coastal areas are experiencing eutrophication due to human-induced nutrient overloading. Algal blooms occur frequently in New Jersey coastal waters, and excessive blooms shift water quality. However, phytoplankton–bacteria interactions mediated through dissolved organic matter (DOM) have not been extensively studied in New Jersey coastal waters, especially near overburdened communities. We targeted a traditionally underrepresented township area, Keyport Harbor, as a model site to investigate seasonal variabilities of phytoplankton biomass, DOM, and bacteria biomass. Chlorophyll-a concentrations were significantly higher in spring–summer (bloom) than in fall–winter (nonbloom). Nitrate + nitrite and ammonium were negatively correlated with chlorophyll-a, and the water was nitrogen-limited during bloom time while phosphorus-limited during nonbloom time, implying that regulating nitrogen loading was key to controlling algal blooms, especially during bloom seasons. Phytoplankton–bacteria interactions were assessed by monitoring dissolved organic carbon (DOC) and bacterial abundance between bloom and nonbloom time from field and incubation studies. A significantly higher DOC, but not dissolved organic nitrogen, occurred in the bloom than nonbloom period, suggesting that phytoplankton contributed to the production of more carbon-rich than nitrogen-rich compounds. DOC fueled threefold bacterial growth in the bloom period, exceeding the temperature effect and indicating strong phytoplankton–DOM–bacteria connections. Microbial remineralization incubations showed rapid phytoplankton–DOC drawdown, and more ambient DOC drawdown and bacterial growth in the bloom than nonbloom time, further supporting the important role of phytoplankton–DOC in shaping bacteria. With water quality monitoring via chemical and biological indicators, the study aimed to understand carbon cycling better, assess anthropogenic impacts on coastal environments, and help facilitate coastal management.

Keywords Coast · Algal bloom · Nutrient · Dissolved organic matter · Microbes

Introduction

Nitrogen and phosphorus are essential nutrients for phytoplankton growth in coastal waters (Ryther and Dunstan 1971). However, excessive nitrogen and phosphorus nutrients in the water lead to eutrophication problems with the rapid reproduction of phytoplankton (algal blooms), which can cause deterioration of water quality such as

high turbidity, depleted dissolved oxygen (DO), die-off of aquatic organisms, and potentially a permanent shift in food web structure (Dorgham 2014). New Jersey coastal waters are susceptible to heavy eutrophication issues due to their proximity to highly urbanized areas with expanding human population, industrial development, agricultural expansion, and associated point and nonpoint sources of pollution (Kennish et al. 2007). For instance, the Barnegat Bay–Little Egg Harbor watershed in mid-New Jersey has shifted its land use to more urbanized coverage, decreasing groundwater recharge and increasing runoff and nutrient loadings since the early 1990s, which turned the bay from a moderately eutrophic system to high eutrophic in three decades, facing consequences including harmful algal blooms, eelgrass and shellfish habitat loss, and diminishing hard clam abundance (Gastrich et al. 2004; Kennish et al. 2007, 2012). Using

✉ Shuting Liu
 liushut@kean.edu

1   Department of Environmental & Sustainability Sciences, Kean University, Union, NJ 07083, USA

2   School of Integrative Science and Technology, Kean University, Union, NJ 07083, USA

the National Estuarine Eutrophication Assessment model, Bricker et al. (2008) showed that one-third of the studied 22 estuaries in the mid-Atlantic region, including New Jersey coastal bays, had worsened eutrophic condition over the survey period from 1990 to 2004, with the most acute effects on shallow coastal lagoons. Although nutrient loading is an important factor of eutrophication, high nutrient levels do not always translate into eutrophication conditions, as top-down grazing and water residence time are also determinants (Heck and Valentine 2007; Kennish 2009). Multiple measurements such as DO, chlorophyll-*a*, and bioindicators are often needed to evaluate eutrophication in addition to nutrients. Therefore, comprehensive studies combining both chemical and biological parameters are needed for management planning.

Algal blooms substantially impact the dissolved organic matter (DOM) dynamics in aquatic environments. Phytoplankton extracellular release accounts for an average of 13.3 Pg C year^{-1} DOC production in the global ocean, far exceeding DOC production from other sources such as zooplankton release and cell lysis (Carlson et al. 2024). As a major source of DOM production in the global ocean, phytoplankton release fresh and labile dissolved organic matter (DOM) into the water, which turns over rapidly, in contrast to the recalcitrant DOM that persists longer (Biddanda and Benner 1997; Hansell 2013; Carlson et al. 2024). Phytoplankton-derived DOM serves as a "bottom-up" control of bacterial growth and production (Buchan et al. 2014). The bacterial population becomes abundant during the peak of algal blooms and immediately following the decline of algal blooms as DOM is released from both healthy and dying phytoplankton (Smith et al. 1995; Grossart et al. 2006; Teeling et al. 2016; Berner et al. 2018). Through bacterial remineralization of DOM, nutrients are regenerated and further support phytoplankton growth. In addition to in situ production by phytoplankton, DOM in coastal waters is also influenced by terrestrial sources such as riverine input. Terrigenous DOM is characterized by higher molecular weight and higher aromaticity (Minor et al. 2006), which is typical of lower bioreactivity and shapes bacterial populations differently from phytoplankton-derived DOM (Blanchet et al. 2017; Xiao et al. 2022). Therefore, the seasonal DOM dynamics and its interaction with bacteria are essential to understanding various biological and physical processes in coastal waters over temporal scales.

Although algal blooms and blooming species have been extensively studied in New Jersey coastal waters (Gastrich 2000; Ren 2013), phytoplankton–bacteria interactions mediated by DOM dynamics and the relationships with water quality from both inorganic and organic perspectives are not well understood yet in this region, especially near overburdened communities with more than 30% low-income population or over 40% minority residents. This study focused on Keyport Harbor, where seasonal changes in phytoplankton biomass were examined to assess their impacts on DOM quantity and quality and their linkages to bacterial dynamics. In addition, microbial remineralization incubation experiments were conducted in this study to investigate the direct utilization of phytoplankton-derived DOM by bacteria while controlling for other environmental factors in Keyport Harbor. Keyport Harbor is located within Raritan Bay, a heavily polluted bay with diatoms such as *Skeletonema costatum* dominant in spring while small flagellates and nonflagellated green algae such as *Didymocystis sp.* dominant in summer (McCarthy 1965; Ryther and Dunstan 1971; Rothenberger et al. 2014). The main streams flowing toward the north and discharging into the bay are Matawan Creek on the northwestern border, Chingarora Creek on the northeastern border, and Luppatatong Creek, which bisects the western portion of Keyport Borough (CME Associates 2007). As an underrepresented area with overburdened communities (NJDEP 2022), it is crucial for Keyport Borough to obtain baseline data on the coastal water quality, including phytoplankton–bacteria interactions, for future coastal management and pollution mitigation plans.

Methods

Study sites and field sampling

Monthly field sampling (between 10 am and 12 pm local time) from April 2023 to March 2024 was conducted along the coast in Keyport Township, NJ (Fig. 1, Table S1). Keyport Harbor is an arm of Raritan Bay that is connected to Sandy Hook Bay in NJ. Four sampling sites at the coast of Keyport Harbor were studied, with site 1 on the western side close to Matawan Creek and Luppatatong Creek that discharge into Keyport Harbor and next to a boat loading dock, site 2 close to a stormwater drainage pipe and community park, site 3 close to a historical landfill site, and site 4 on the eastern side close to Chingarora Creek that discharges into Keyport Harbor. The exact location of site 4 (4–1, 4–2, and 4–3) varies over time owing to beach accessibility influenced by seasonal tidal levels; however, it was always close to the river mouth of Chingarora Creek.

The surface (within top 0.5 m) water temperature was recorded by using a thermometer, salinity was monitored by a refractometer, pH was measured by a pH meter (Thermo Scientific), and dissolved oxygen (DO) was analyzed using the Winkler titration method (LaMotte DO water test kit). Surface water with a 300–500 mL volume was filtered onto precombusted (450 °C for 4.5 h) GF/F (Whatman, nominal pore size of 0.7 μm) filters under a low vacuum pressure (< 15 inHg) and stored at −20 °C for chlorophyll-*a* analysis. Water (30 mL) was syringe filtered through 0.45-μm-pore-size
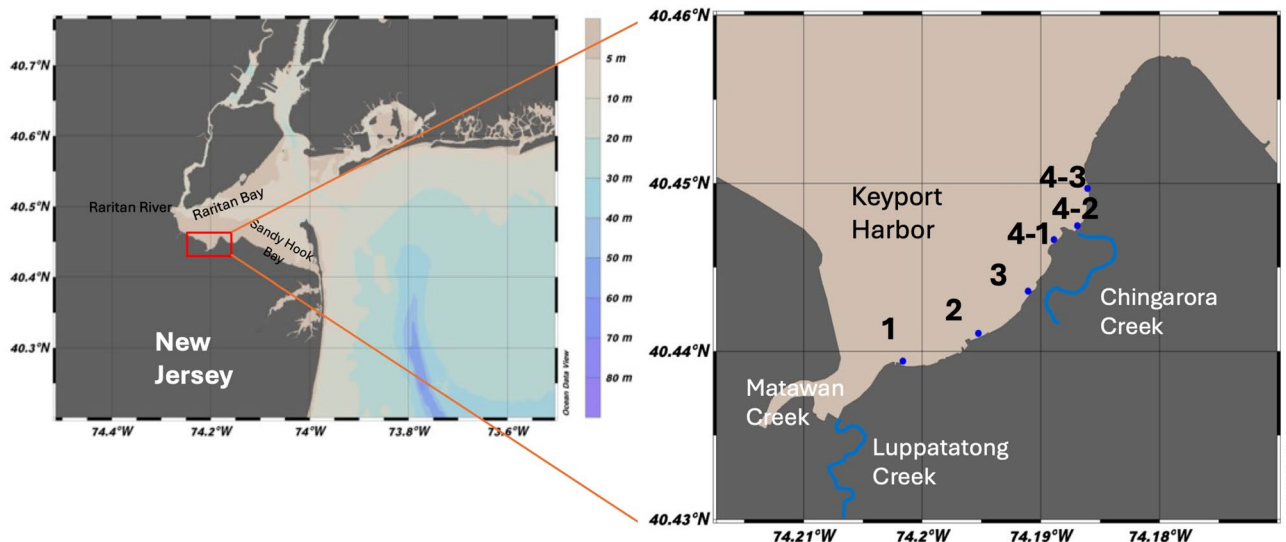
Fig. 1 Map showing sample locations in Keyport Harbor, NJ. Site 1 is close to Matawan Creek and Luppatatong Creek and next to a boat loading dock, site 2 is close to a stormwater drainage pipe and community park, site 3 is close to a historical landfill site, and site 4 is near the river mouth of Chingarora Creek. The exact location of site 4 (4–1, 4–2, and 4–3) varies over time owing to beach accessibility influenced by seasonal tidal levels

polyethersulfone filters into acid-cleaned high-density polyethylene (HDPE) bottles as nutrient samples and stored at −20 °C before analysis. Another 30 mL of water was filtered through precombusted GF/F filters into precombusted 40-mL borosilicate glass vials with polytetrafluoroethylene (PTFE)-coated silicone septa and acidified to pH ~3 with HCl for dissolved organic carbon (DOC) and total dissolved nitrogen (TDN) analysis. For bacterial abundance, 10 mL water was collected in sterile tubes (Falcon™), fixed with 1% formalin, and preserved at −80 °C until analysis.

Chlorophyll-*a* analysis

Phytoplankton chlorophyll on GF/F filters was extracted twice (second-time extraction in case of residual chlorophyll on the filter after first-time extraction) with 4–6 mL 90% acetone under sonication for 15 min. Extracts were filtered through 0.2-µm-pore-size Nylon syringe filters and measured before and after acidification at fixed wavelengths of both 665 nm (chlorophyll-*a* maximal absorbance) and 750 nm (to correct for turbidity) wavelength on a ultraviolet–visible (UV–Vis) spectrophotometer (Agilent 8453) to determine chlorophyll-*a* concentrations from technical duplicates (Lorenzen 1967). Chlorophyll-*a* concentrations were calculated using the equation

$$\text{Chlorophyll-}a = \frac{A \times K \times (665_0 - 665_a) \times v}{V_f \times l},$$

where *A* is the absorbance coefficient derived from a standard curve, *K* is the factor to equate reduced absorbance to initial chlorophyll concentration due to acidification, which is a constant value of 1.7:0.7, 665_0 is the absorbance before acidification with turbidity correction, 665_a is the absorbance after acidification with turbidity correction, *v* is the volume of acetone used for extraction, V_f is the total volume of filtered water sample, and *l* is the path length of the cuvette. Occasional (6% of samples) duplicates of chlorophyll-*a* samplings showed an average variation of ~4%.

Nutrient analysis

Nitrate + nitrite concentrations were measured on the spectrophotometer on the basis of the absorbance at a wavelength of 543 nm after cadmium reduction (Jones 1984). Soluble reactive phosphate concentrations were analyzed at 880 nm on the spectrophotometer following the ascorbic acid method and reaction with ammonium molybdate (Strickland and Parsons 1968). Ammonium concentrations were analyzed by using a fluorometer (Hitachi F-2000, Ex = 360 nm, Em = 420 nm) following the *o*-phthaldialdehyde derivation method (Holmes et al. 1999). Technical duplicates were obtained for each sample. Occasional (6% of samples) duplicate samplings of nutrients showed average variations of ~10%.

DOC and DON analysis

DOC and TDN concentrations were measured using high-temperature combustion by a TOC-L analyzer with TNM (Shimadzu) with a coefficient of variation (CV) of ~2% (Halewood et al. 2022). Glucose and potassium nitrate standards were used for carbon and nitrogen calibration, respectively. In-house reference water collected from Key-port and consensus reference material reference water from D. Hansell (University of Miami) were included in the run for between-batch calibration. Occasional (6% of samples) duplicates of DOC and TDN sampling revealed a ~2% variation. DON was calculated as the difference between TDN and inorganic nitrogen (i.e., nitrate + nitrite and ammonium).

Total bacterial abundance analysis

One mL of water from bacterial samples was filtered onto Irgalan black-stained 0.2 µm polycarbonate filters under a gentle vacuum. Cells on filters were then stained with 5 µg mL^{-1} 4′,6′-diamidino-2-phenylindole dihydrochloride (Sigma-Aldrich) and mounted onto slides with high-viscosity immersion oil (Porter and Feig 1980). Bacterial cells were enumerated under UV excitation using an epifluorescence microscope (Leica DM4 B) at 1000× magnification. At least ten fields per slide were captured on images and analyzed using ImageJ (Stephens et al. 2020). Note that bacteria attached to particles are also captured in images (Fig. S1). Occasional (6% of samples) duplicate samples of total bacterial counts were within 11% variation.

Microbial remineralization experiments

To further test the direct relationships between phytoplankton-derived DOM and bacteria by controlling other environmental factors, water from site 2 was collected for setting up microbial remineralization experiments in August and November 2023. Upon collection, water was prefiltered through 11-µm-pore-size filters to reduce large particles, phytoplankton, and grazers (Nielsen and Kiørboe 1991) and focus on heterotrophic bacterial utilization of DOM. Although 11-µm filters cannot exclude all grazers, they can greatly dilute them and limit their functions in the incubation without totally losing particle-attached bacteria in the natural water. In each experiment, two treatments with duplicates were included, including a control treatment with 11-µm filtrate only and an amendment treatment with 10 µM C (target concentration) algal lysate DOM added to the 11-µm filtrate. Algal lysate DOM was harvested from *Thalassiosira weissflogii* cultures (CCMP1336) growing under a 14/10 light/dark cycle at 14 °C (following Bigelow Laboratory protocols) upon centrifugation, cell lysis with bead beating, and filtration of extracts through 0.2-µm filters (Liu et al. 2020).

Thalassiosira weissflogii is a coastal diatom species, and diatoms account for up to 75% of primary production in the coastal water (Nelson et al. 1995). Microbial remineralization experiments were conducted in the dark at room temperature (17–20 °C, similar temperature between August and November to rule out temperature effects) for 14–15 days to capture rapid drawdown of DOM by bacteria. During the incubation, aliquot samples were collected for DOC and bacterial abundance analysis as described above.

Data analysis and plotting

The sampling map and spatial data on various parameters were plotted using Ocean Data View (version 5.6.2) (Schlitzer 2022). Comparison between groups of data on the basis of main factors of month and site were conducted using the nonparametric Friedman test (accounted for data nonnormality and corrected for unequal variance using Greenhouse–Geisser correction), and pairs with significant differences were identified with follow-up Dunn's multiple comparisons. Boxplots together with statistical t-test comparison results were plotted using R (version 4.2.1) with the ggplot2 (Wickham 2016) and ggpubr packages (Kassambara 2023). The Pearson correlation and correlation heatmap on all variables were generated using R packages Hmisc (Harrell Jr. and Dupont, 2019), car (Fox and Weisberg 2019), reshape2 (Wickham 2007), and ggplot2. Temporal changes were fit by using sinusoidal regression with the nls function in R, and the Pearson correlation between the fit curve and data was assessed.

Results

Environmental conditions at sampling sites

The temperature, salinity, DO, and pH at the four sampling sites showed significant seasonal variations, with the highest temperature and lowest DO in summer, lowest salinity in spring (March), and highest pH in spring (May) (Table S1, S2). Temperature and DO exhibited a significant negative correlation ($p = 0.0119$, Supplementary Fig. S2). The salinity, ranging from 10 to 27 ppt, indicates a brackish water body. The lowest salinity in March occurred after three successive rainfall events combined with high surface current speed that brought freshwater toward the bay in spring (Supplementary Fig. S3, S4). Between sampling sites, no significant difference was observed for DO and pH. In contrast, significant differences in temperature and salinity were observed only between site 2 and site 4 and between site 1 and site 4, respectively (Dunn's test, $p < 0.05$, Supplementary Table S2), potentially owing to site 4 being near the river mouth mostly influenced by the freshwater.

Chlorophyll-*a* and nutrient variations

Chlorophyll-*a* concentrations ranged over a fivefold difference over temporal scale, with the lowest value of 0.7 μg L^{-1} in December and the highest value of 30.5 μg L^{-1} in July (Fig. 2a, Supplementary Fig. S5a). Chlorophyll-*a* showed seasonal variations with higher values in March–September compared with other months. Data here and in the following were thus grouped into bloom (March–September) and nonbloom (October–February) periods. The nonparametric test showed a significant difference among both months ($p < 0.0001$) and sites ($p < 0.05$) (Fig. 2b, Supplementary Table S2). An abnormally low concentration of chlorophyll-*a* occurred in June during the bloom period.

Corresponding to the chlorophyll-*a* seasonal pattern, nitrogen nutrients (nitrate + nitrite) and ammonium concentrations in the bloom period were significantly lower than in the nonbloom period; however, phosphate concentrations showed an opposite pattern between the two periods (Fig. 3). Concomitant with the significant difference of chlorophyll-*a* used to categorize the bloom and nonbloom groups, nutrients showed statistical difference among seasons and opposite seasonal patterns between chlorophyll-*a* and nitrogen nutrients (Fig. 4). Average nitrate + nitrite concentrations in the nonbloom season (43.4 ± 11.8 μmol L^{-1}) were 1.5 times those in the bloom season (26.9 ± 13.8 μmol L^{-1}), and average ammonium concentrations in the nonbloom season (24.4 ± 6.7 μmol L^{-1}) were 2.5 times those in
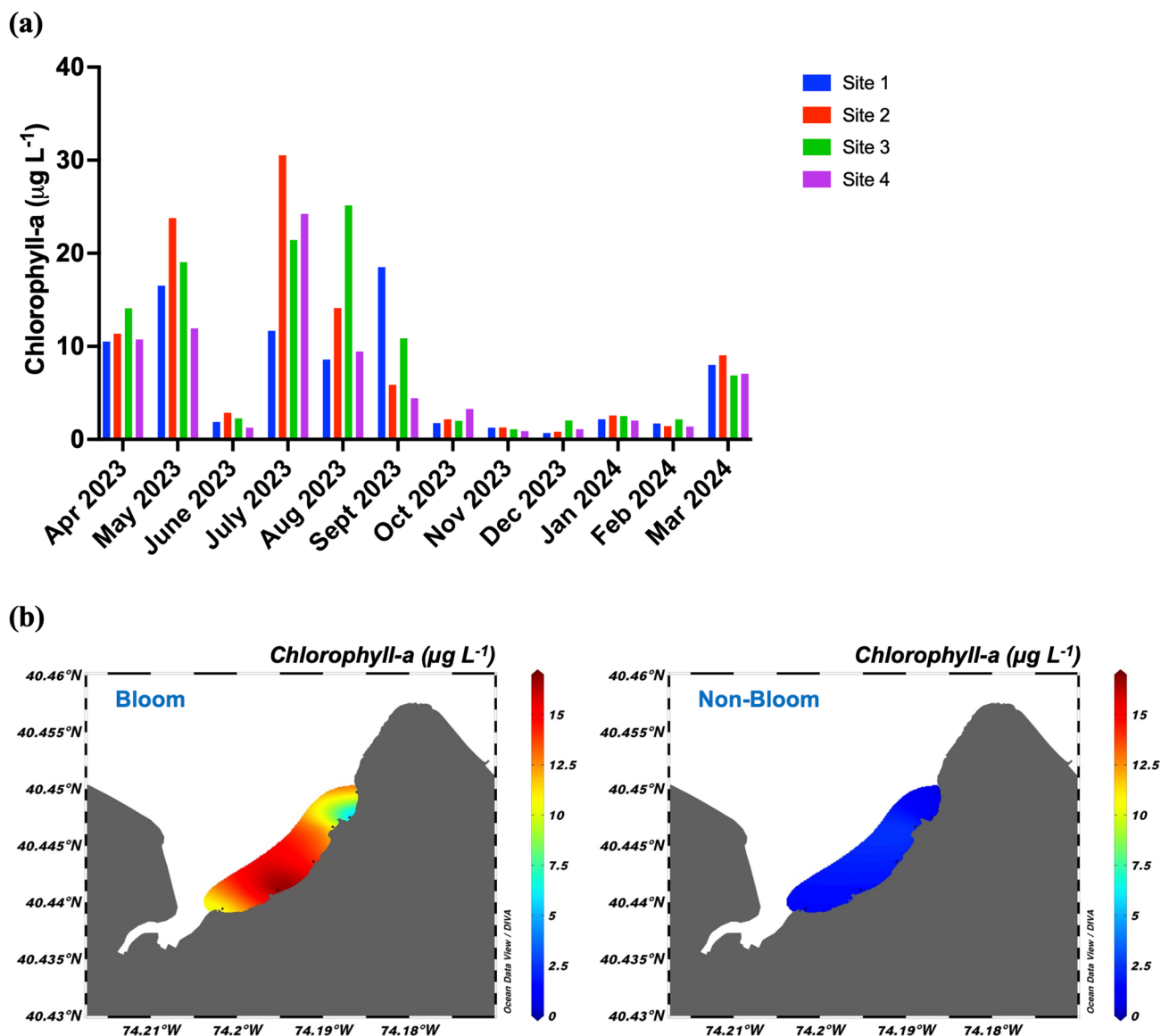
Fig. 2 **a** Seasonal variations in chlorophyll-*a* concentrations at four sampling sites. **b** Ocean Data View (ODV) contour plots of averaged chlorophyll-*a* concentrations between bloom (March–September) and nonbloom (October–February) seasons

(a)

(b)

(c)
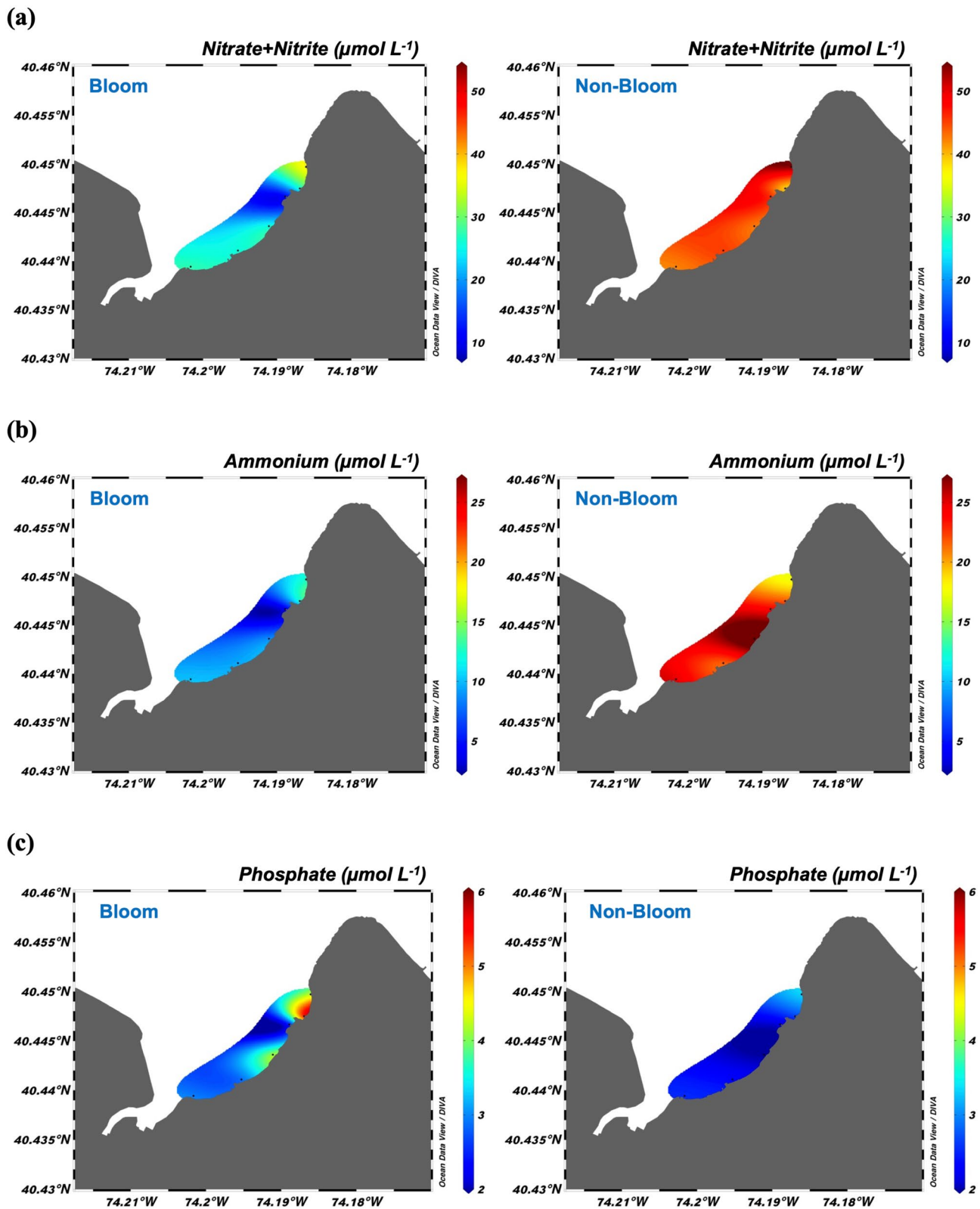
Fig. 3 ODV contour plots of averaged nitrate + nitrite (**a**), ammonium (**b**), and phosphate (**c**) concentrations between bloom (March–September) and nonbloom (October–February) seasons

Fig. 4 Boxplots of chlorophyll-*a* (**a**), nitrate + nitrite (**b**), ammonium (**c**), and phosphate (**d**) concentrations at four sampling sites in bloom (March–September) and nonbloom (October–February) seasons. Asterisks indicate a significant difference between bloom and nonbloom seasons (****$p < 0.0001$), while ns indicates no significant difference
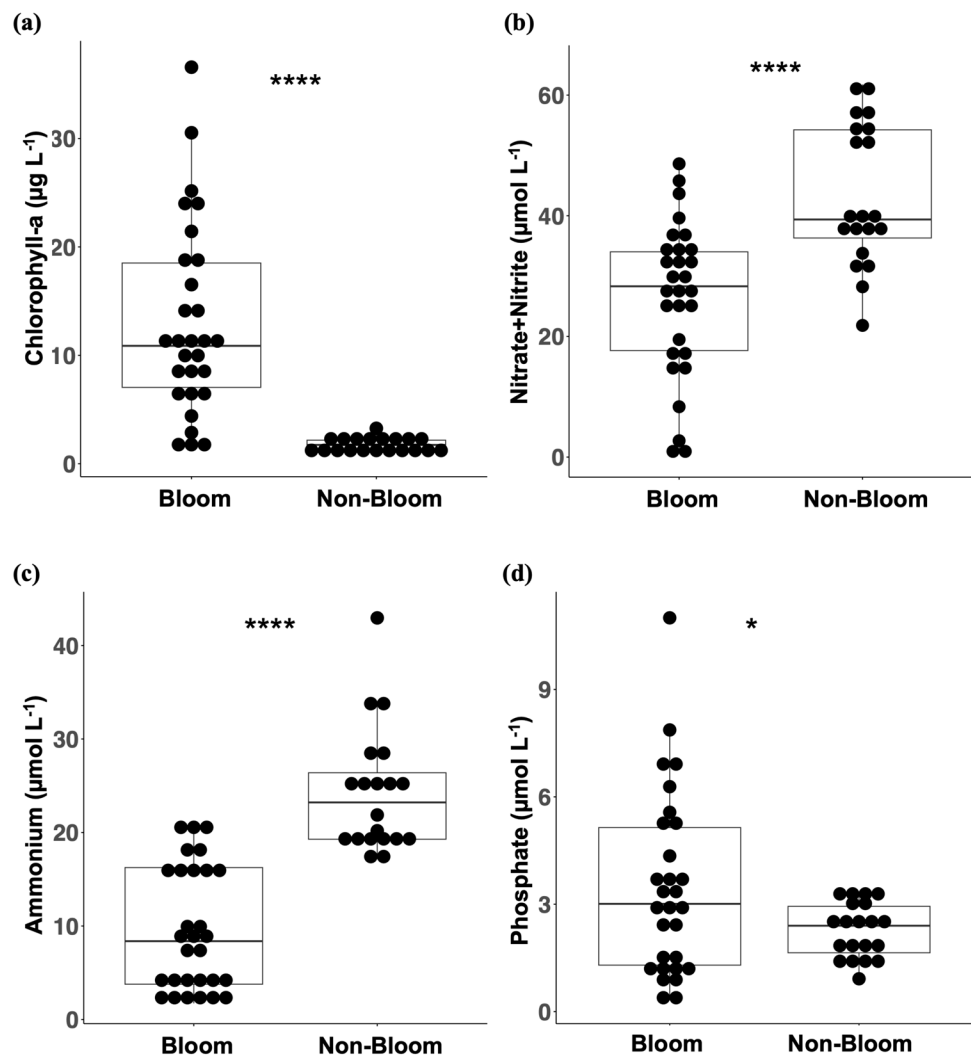
the bloom season (9.7 ± 7.3 μmol L^{-1}). Gradual increase of nitrate + nitrite and ammonium concentrations from July to September within the bloom season corresponded to chlorophyll-*a* shift from peak to declining bloom period (Supplementary Fig. S5a–c, Fig. 2). The highest concentration of nitrate + nitrite occurred in October, and that of ammonium occurred in Feb, whereas the highest concentration of phosphate occurred in June (Supplementary Fig. S5b–d). Nonparametric analysis revealed only temporal differences for nutrients, with no spatial differences among sites (Supplementary Table S2).

DOM and bacterial abundance patterns

DOC showed both temporal and spatial variations, with significantly higher concentrations in the bloom period than in the nonbloom period (Fig. 5a, c, Supplementary Fig. S5e) and significant differences among sites (Fig. 5a, Supplementary Table S2). DOC stayed constantly high in the bloom time, averaging 253.6 ± 28.4 μmol L^{-1} and

205.7 ± 36.7 μmol L^{-1} in the bloom and nonbloom period, respectively. Significant differences in DOC among sites were found between site 1 and site 4, between site 2 and site 4, and between site 3 and site 4. In contrast, DON concentrations did not differ significantly between bloom and nonbloom periods (Fig. 5b), although a difference existed between individual months (Supplementary Table S2, Supplementary Fig. S5f). No significant difference among sites was associated with DON concentrations.

Corresponding to the DOC and chlorophyll-*a* pattern, bacterial abundance in the bloom period was three times as high as in the nonbloom period, contributing to the significant temporal difference (Fig. 6, Supplementary Table S2). No obvious spatial difference in bacterial abundance was observed. The highest bacterial abundance occurred in May, and the bacterial abundance ranged from 1.8×10^6 to 2.3×10^7 cells mL^{-1} in the bloom season, in comparison with 1.1×10^6–8.4×10^6 cells mL^{-1} in the nonbloom season (Supplementary Fig. S5g).

(a)

(b)

(c)
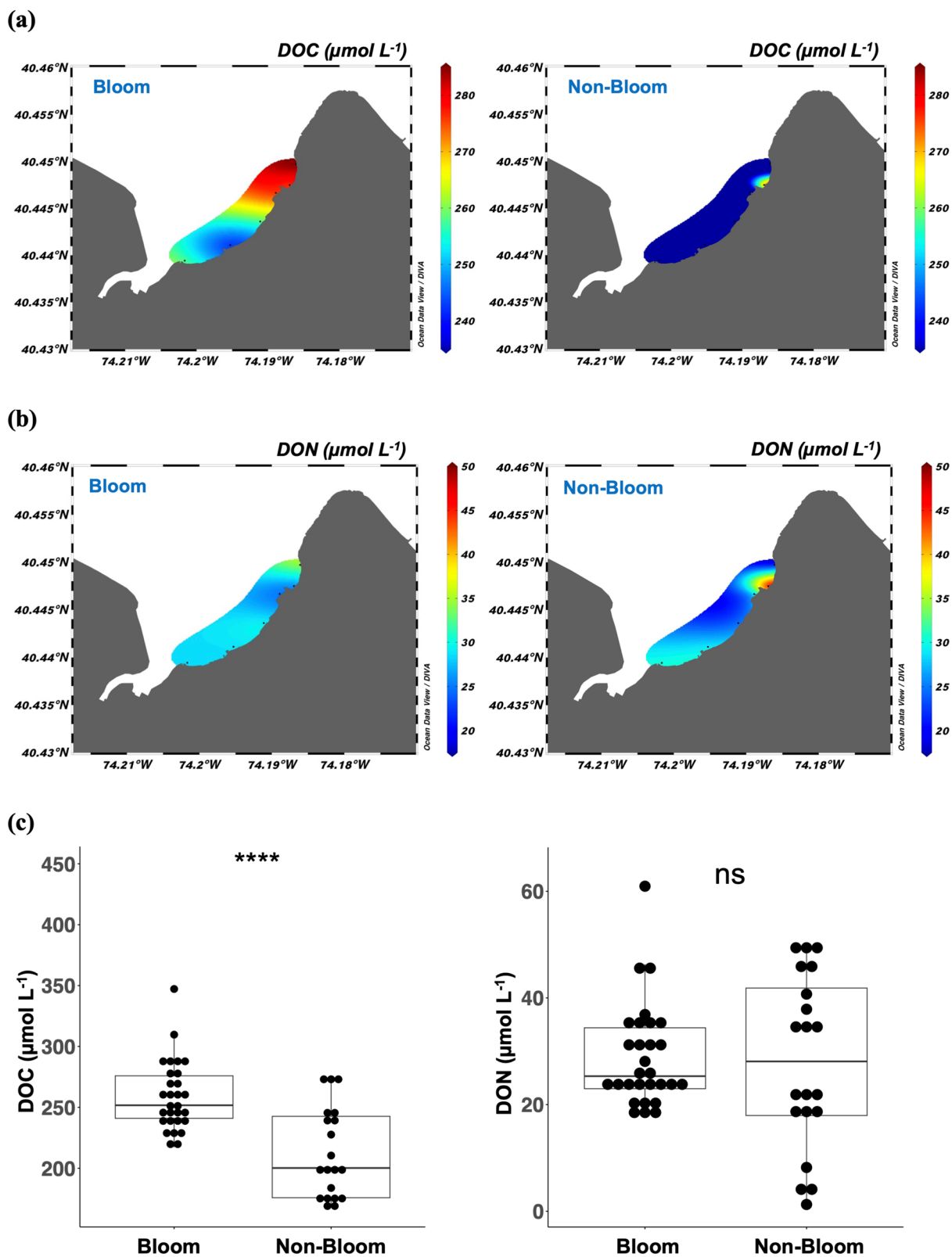
Fig. 5 Contour plots of DOC (**a**) and DON (**b**) concentrations between bloom (March–September) and nonbloom (October–February) seasons. **c** Boxplots of DOC and DON at four sampling sites in bloom and nonbloom seasons. Asterisks indicate a significant difference between bloom and nonbloom seasons (***$p < 0.001$), while ns indicates no significant difference

(a)

(b)
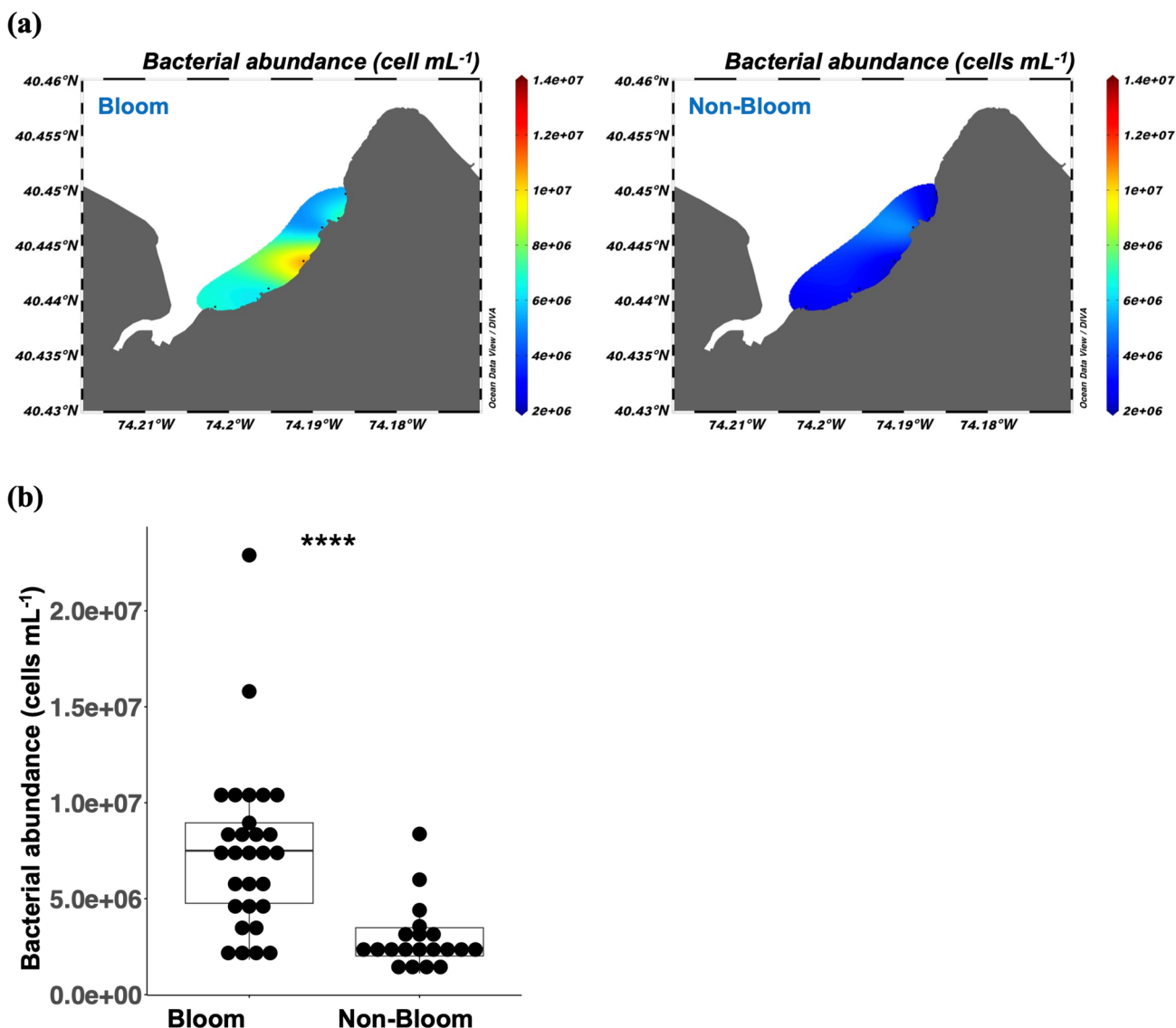
Fig. 6 a Contour plots of bacterial abundance between bloom (March–September) and nonbloom (October–February) seasons. **b** Boxplots of bacterial abundance at four sampling sites in bloom and nonbloom seasons. Asterisks indicate a significant difference between bloom and nonbloom seasons (****$p < 0.0001$)

Microbial remineralization experiment results

Consistent with bloom versus nonbloom patterns, DOC started at a higher concentration in the bloom period at the initial time point of the incubation experiments (Fig. 7). During the ~2-week incubation, there was 71 µmol L^{-1} DOC drawdown in the control treatment during the bloom time, accounting for 19% removal of the initial DOC. However, during the nonbloom time, lower DOC drawdown (26 µmol L^{-1}) and percent removal (11%) were observed in the control treatment (Fig. 7a, b). In the phytoplankton lysate amended treatment, DOC addition in the bloom time exceeded the targeted 10 µmol L^{-1}, possibly owing to particulate dissolution to the 11-µm filtrate during the filtration preparation process

(as filtrate for control treatments was prepared before that for amendment treatments, more accumulate of dissolution from the same filter might carry over more DOC to the amendment treatments). However, all amended lysate DOC was removed within the first 1–2 days in both bloom and nonbloom periods in the lysate treatment. Similar to the control treatment, the DOC removal percentage in the bloom time in the lysate treatment was twice as high as that in the nonbloom time.

Bacterial abundance in the incubation also showed distinct patterns between bloom and nonbloom time. Comparing two control treatments between seasons, while bacteria grew twofold during the first 4 days and then declined in the control treatment during the bloom period, their abundance

Fig. 7 a DOC drawdown in the control and algal lysate treatment over the microbial remineralization incubation conducted in August and November during bloom and nonbloom seasons, respectively. Note the *y*-scale difference between the two plots. **b** DOC removal % from initial to end of incubation (14–15 days) in two incubations. **c** Bacterial abundance changes over time in two incubations
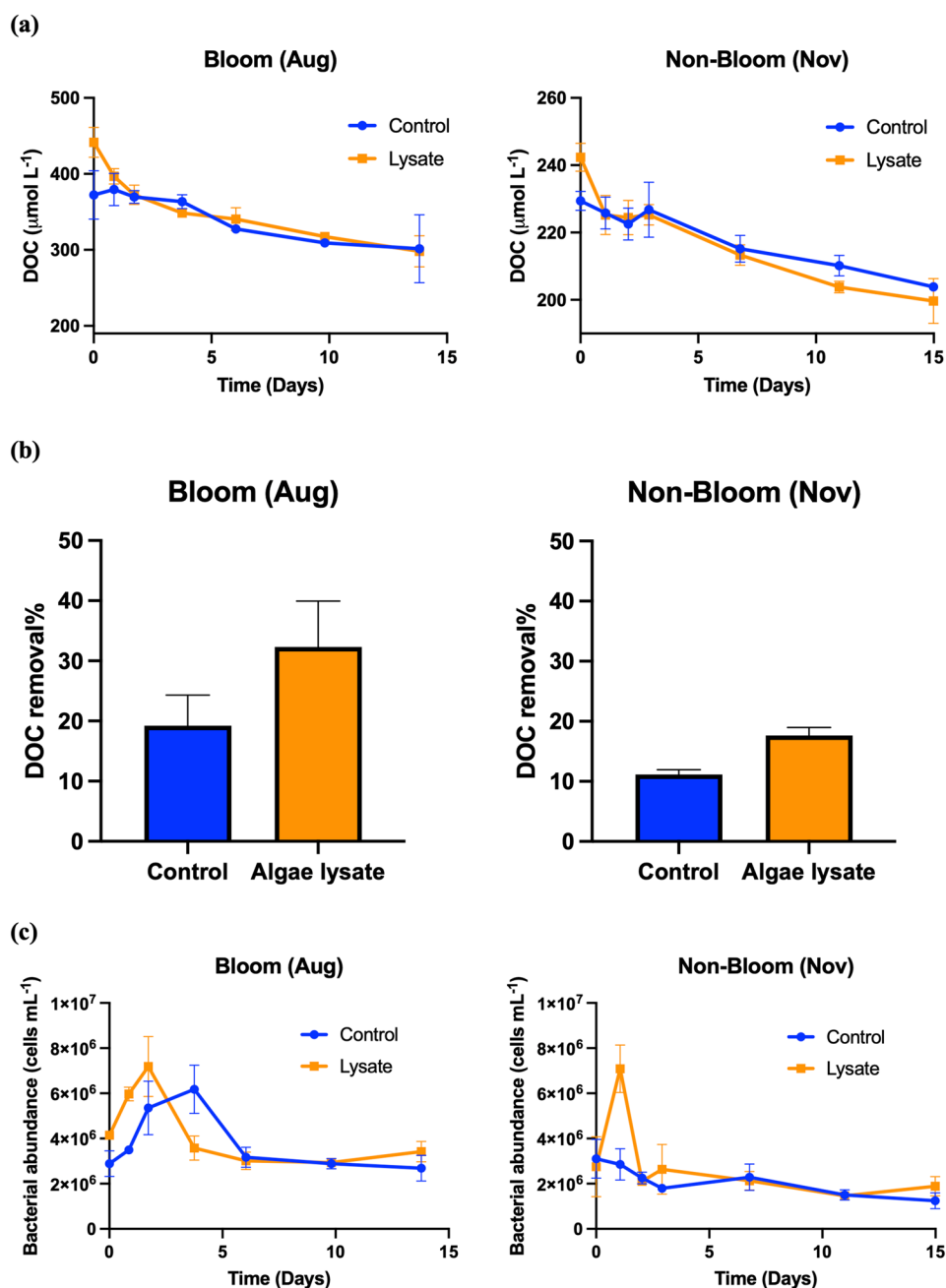
decreased over the entire incubation in the control treatment during the nonbloom period (Fig. 7c). Bacteria abundance peaked within 1–2 days, matching the removal time of amended lysate DOC, reached similar maximal counts, and then decreased in the lysate treatment during both times. Note that the water for microbial remineralization experiments was prefiltered through 11-µm filters to reduce large particles and grazer effects, which excluded some large particle-attached bacteria, leading to lower bacterial abundance at the starting point of the incubation compared with the total bacterial abundance in the field sample above, which focused on total counts in the whole water.

Discussion

According to the State of New Jersey water quality standards, ammonium concentration in the coastal seawater should not exceed 1.3 µM (0.024 mg/L) as the chronic toxicity level (adverse impacts on the growth, survival, or reproductive success of an organism or its progeny after long-term exposure) and 5.2 µM (0.094 mg/L) as the acute toxicity level (lethal or sublethal impacts on an organism after short-time exposure), and total phosphorus concentration should be less than 0.003 µM (0.1 µg/L) at the chronic toxicity level (EPA 2016). In our study, all samples exceeded the total

phosphorus quality standard and ammonium chronic toxicity level, and samples from 8 out of 12 months exceeded the ammonium acute toxicity level (Fig. 4), indicating that Keyport Harbor water is a highly contaminated and unhealthy coastal environment to aquatic life, and highly eutrophic to support algal bloom events, consistent with the results from the previous study on the larger scale in the Raritan Bay showing pollution by urban development and industrialization (Jeffries 1962; Bagheri 2017). Algal blooms in the Keyport water started as early as in March during spring and peaked in the warm months in summer, showing a significantly positive correlation between temperature and chlorophyll-*a* with both bloom and nonbloom data pooled together (Fig. 8). In addition to the temperature factor, the correlation heatmap also showed a significant negative correlation between chlorophyll-*a* and nitrate + nitrite, and between chlorophyll-*a* and ammonium (Fig. 8), suggesting that phytoplankton took up inorganic nitrogen in Keyport Harbor water and inorganic nitrogen was an important factor in phytoplankton growth in this water body. No significant correlation between chlorophyll-*a* and phosphate indicates surplus phosphate or phosphate regeneration in the water

during the bloom period. Unlike nitrogen, phosphorus absorbs onto colloids and suspended particles, which settle to remove it from biological processes until detritus feeders release phosphorus from sediments back into the water column in the summertime when bacterial activity is high (Jeffries 1962). In addition, bacteria produce enzymes to convert organic phosphorus to inorganic phosphate (Sylvan and Ammerman 2013). Digestion of dead plankton promotes the regeneration of phosphate through high bacterial activities in the summer, leading to a different phosphate seasonal cycle compared with inorganic nitrogen. The high phosphate concentrations (Fig. 4d) and bacterial abundance in the bloom period in this study (Fig. 6) supported the above hypotheses.

The dissolved inorganic nitrogen (DIN, i.e., the sum of nitrate + nitrite and ammonium) and dissolved inorganic phosphorus (DIP, i.e., phosphate) concentrations in this study (Table 1) align with the range in recent studies on Raritan Bay and Raritan estuaries, although some include nitrate only in DIN (Maest et al. 1990; Rothenberger et al. 2014). However, earlier studies in the 1950s revealed much lower nutrient concentrations in Raritan Bay (Jeffries 1962), together with other evidence of persistent high

Fig. 8 Pearson correlation heatmap between all variables (including both bloom and non-bloom data). The color indicates the correlation coefficient. Correlation coefficient values and significance levels (*$p < 0.05$, **$p < 0.01$; ***$p < 0.001$, ****$p < 0.0001$) are indicated in each cell
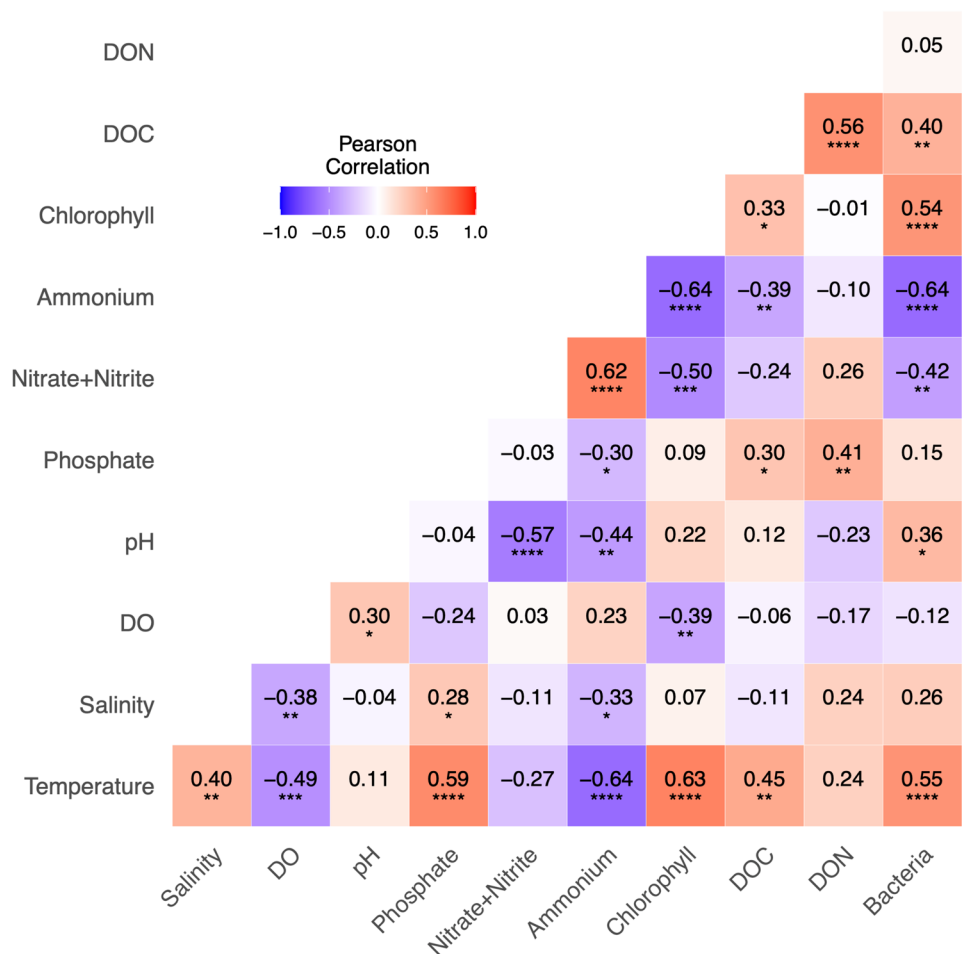
Table 1 DIN concentration, DIP concentration, and DIN/DIP ratio (average ± standard deviation or range) in this study compared with surface waters from other studies in estuaries and bays near New Jersey

Region	Time	DIN (µmol L^{-1})	DIP (µmol L^{-1})	DIN/DIP	References
Chesapeake Bay, MD	1945–2012	83.57 ± 1.43[a]	< 0.5 to > 2	< 2 to > 120	(Harding et al. 2016)
Georges Bank, MA	1930–1940	0.41 ± 0.13[b]	0.026 ± 0.0092	17.3 ± 6.3	(Riley 1941)
Delaware Bay, DE	1974–1975	0.61 ± 0.44	0.0066 ± 0.0091	146.7 ± 182.6	(Maurer et al 1978)
Narragansett Bay, RI	1985–1987	1.35 ± 1.26	0.077 ± 0.045	6.6 ± 3.0	(Smayda and Borkman 2008)
Long Island Sound, NY	1952–1954	0–1.57[b]	0.0065–0.14	< 22	(Riley and Conover, 1956)
Great South Bay, NY	1998–1999	0–26	< 0.15 to < 2	~2.5	(Clark et al. 2006)
Great South Bay, NY	1999	2.52 ± 1.88	0.34 ± 0.21	9.7 ± 8.7	(Gobler et al. 2002)
Hudson River Estuary, NY	1973–1978	61.34 ± 18.40	0.30–6.20	7.6–204	(Deck 1981)
Barnegat Bay, NJ	2014–2015	2.22 ± 2.06	0.79 ± 0.66	1.8 ± 1.0	(Paudel et al 2017)
Raritan estuaries, NJ	1982	58-110[b]	0–20	4.76–49.77	(Maest et al. 1990)
Raritan Bay, NJ	1957–1958	2.44 ± 2.28[b]	0.093 ± 0.027	1.3–111.4	(Jeffries, 1978)
Raritan Bay, NJ	2010–2012	54.01 ± 15.57[b]	1.58 ± 0.43	35.4 ± 10.9	(Rothenberger et al. 2014)
Keyport Harbor, NJ	2023–2024	46.06 ± 24.50	2.94 ± 2.05	23.8 ± 20.9	This study

[a]Nitrate + nitrite only; [b]nitrate only

phytoplankton biomass, high turbidity, and harmful phytoplankton species in more recent times (Rothenberger et al. 2014, 2023), suggesting that the eutrophication problem has become exacerbated in the bay. Nutrient levels in our study fall in the range detected in Raritan estuaries around the 1980s (Table 1) (Maest et al. 1990). Compared with other estuaries and bays nearby, nutrient concentrations in Keyport Harbor were close to those in the Chesapeake Bay and Hudson River Estuary (Deck 1981; Harding et al. 2016), and higher than ecosystems such as George Bank, Delaware Bay, Narragansett Bay, Long Island Sound, Great South Bay, and Barnegat Bay (Riley 1941; Riley et al. 1956; Maurer et al. 1978; Gobler et al. 2002; Clark et al. 2006; Smayda and Borkman 2008; Paudel et al. 2017), implying a need to mitigate excessive nutrients in the Keyport coastal waters. The DIN/DIP ratio in this study averaged 23.8 ± 20.9, with seasonal variations of DIN/DIP below the average Redfield ratio of 16:1 during May to Aug in the bloom period and DIN/DIP above the average Redfield ratio in other months (Supplementary Fig. S6, Table 1). This indicates that Keyport Harbor water was nitrogen-limited during summer bloom periods and phosphorus-limited during non-bloom periods. Rivers are important nutrient sources to Raritan Bay and discharge nitrogen and phosphorus during the wet spring season (Jeffries 1962), triggering the initial start of algal bloom (Fig. 2, Supplementary Fig. S3). Reduction of riverine input during the dry summer season, together with the phosphate regeneration by bacterial activities, leads to the used-up DIN, build-up DIP, and low DIN/DIP in the summer bloom time (Supplementary Fig. S6). Seasonal variations of nutrients and DIN/DIP ratio were also consistently shown in other coastal studies on various ecosystems (He et al. 2023; Wang et al. 2024). In response to the Environmental

Protection Agency's requirement for total maximum daily loads (TMDLs), TMDLs established in the Raritan River Basin, which discharge into the Raritan Bay, have been focused mainly on total phosphorus (NJDEP 2016), with nitrate TMDLs for a few sites (Kleinfelder 2013). However, our study revealed a need to regulate nitrogen loading to control algal blooms, especially during the bloom seasons. Ryther and Dunstan (1971) also showed that nitrogen is the critical limiting factor for controlling eutrophication and algal growth in the coastal environment and removing phosphate from detergents is not enough to solve the eutrophication problems in coastal waters. Located in the understudied region of Raritan River Basin (Kleinfelder 2013), Keyport Borough, with dominant urban residential land use around managed wetlands (CME Associates 2007), lacks a region-specific management plan for both nitrogen and phosphorus in the coastal water, and this study provides scientific evidence.

Different species of nitrogen nutrients, such as nitrate + nitrite and ammonium, were taken up by phytoplankton during the bloom period in Keyport Harbor (Fig. 8), suggesting either a switch of nitrogen species uptake by the same phytoplankton upon nutrient concentration variation or multiple phytoplankton groups capable of utilizing different nitrogen species simultaneously present in the water. Nitrate has a higher energy requirement for uptake than ammonium, and phytoplankton species tend to take up nitrate as a nitrogen nutrient only when the ammonium concentration becomes lower than 1–2 µmol L^{-1} (Miller 2004), which might lead to dual nitrogen species use over a broad time scale, as observed here. Alternatively, species differences play a role in the preference for nitrate versus ammonium (Dortch 1990). Seasonal variations in

nitrate and ammonium preference by coastal phytoplankton have been observed (Collos et al. 2003). Diatoms were found to have a higher nitrate uptake rate than flagellates in culture studies (Lomas and Glibert 2000). Flagellates, chlorophytes, diatoms, and cyanobacteria are the major phytoplankton groups in Raritan Bay (Rothenberger et al. 2023), suggesting that different species were present and might play a role in the uptake of both nitrogen species. More studies on phytoplankton community composition over finer time resolution in the Keyport water are needed to further distinguish between the two mechanisms. Nitrate is often considered to support new production, in contrast to regenerated production from the uptake of recycled nutrients such as ammonium. The f-ratio, the proportion of total primary production supported by nitrate, is usually much less than 0.5 in coastal estuaries unless external nitrogen input from rivers peaks (Crump and Bowen 2024). Assuming that the average change of nitrate + nitrite and ammonium between the non-bloom and bloom periods was solely due to algal uptake and supports the algal production in the Keyport Habor water, a coarse estimate of f-ratio in this study was 0.53, suggesting a considerable amount of external input of nitrogen in this system and the need to pay attention to various nitrogen species in the New Jersey coastal water.

As the aquatic life protection criterion, the DO in coastal water should not be less than 5.0 ppm, and turbidity should not exceed 10 NTU on the basis of the State of New Jersey water quality standards (EPA 2016). The DO in our studied Keyport Harbor water was mostly above 5.0 ppm, with occasional lower values in the hot summertime (Table S1). However, algal blooms may exacerbate the low-oxygen situation in the summer when dead phytoplankton are degraded by bacteria. Although turbidity was not consistently monitored in this study, a buoy deployed in Keyport Harbor reported a turbidity of > 10 NTU 88% of the time during June–October 2023 (Supplementary Fig. S7), suggesting low water quality in terms of turbidity in Keyport Harbor. In addition to the algal blooms that increase water turbidity, high pulses of turbidity in Keyport Harbor also come from creeks, rivers, and storms. Both Matawan Creek and Chingarora Creek, located within Keyport Borough, are identified as substandard for supporting aquatic life, such as macroinvertebrates, or primary contact recreation, indicating high pollutants and low water quality in the water discharging into the harbor (CME Associates 2007). Coinciding with tropical storm Lee (5–18 September 2023) and Ophelia (21–26 September 2023), the turbidity in Keyport Harbor peaked at > 25 NTU and > 75 NTU, respectively (Supplementary Fig. S7). With the current circulation from eastern offshore to west in northern Raritan Bay, protruding with eddies and freshwater discharge from Raritan River, and moving seaward towards east in southern Raritan Bay (including Keyport Harbor) (Jeffries 1962), Keyport Harbor water is connected with surrounding aquatic ecosystems. Coherent monitoring of water quality baseline and algal blooms associated with eutrophication in the Keyport Harbor coastal water is crucial to coastal management and coping with future changes in the New Jersey coast.

Intriguingly, chlorophyll-*a* concentrations were abnormally low in the June samples during the bloom season (Fig. 2a). As salinity did not change significantly in June (Tables S1, S2) and nutrients were replete in that month (Supplementary Fig. S5), the possibility of different water mass or nutrient limitation that results in a drop of chlorophyll-*a* was minimal. This low value was likely attributed to the wildfire in Canada that occurred over 6–8 June 2023, which brought smoke and ash to the New Jersey coastal water that is on the track of the smoke trajectory (Dong et al. 2023). Turbidity consistently increased up to 25 NTU around the June sampling time in Keyport Harbor (Supplementary Fig. S7), which might have resulted from ash deposition and posed a slight limitation on algal growth in June. Alternatively, toxic substances in wildfire smoke and ash, including various hazardous air pollutants, polycyclic aromatic hydrocarbons, and some metals, may have an influence on water chemistry and algal growth (O'Dell et al. 2020; Gomez Isaza et al. 2022; Paul et al. 2022). However, more studies are needed to pinpoint the exact reason for this abnormal chlorophyll-*a* signal.

Phytoplankton and bacteria exhibit complex direct or indirect interactions, such as through particle association or via excretion of DOM. Typical mutualism relationships form between phytoplankton and bacteria, with bacteria providing micronutrients such as vitamins (Bertrand et al. 2015), iron (Amin et al. 2009), and signaling chemicals for cell division (Amin et al. 2015) to phytoplankton, while phytoplankton excrete organic matter for bacterial utilization. Chlorophyll-*a* is usually employed as an indicator for phytoplankton biomass, which affects the variability of bacterial richness and production (Pinhassi et al. 2004; Camarena-Gómez et al. 2021). The significant positive correlation between chlorophyll-*a* concentration and bacterial abundance in this study suggests a tight coupling between phytoplankton and bacteria in the Keyport water (Fig. 8). While particle association can be an important driver of phytoplankton–bacteria interactions (Arandia-Gorostidi et al. 2022), the interaction mediated through DOM produced by phytoplankton is often easily overlooked. This study specifically assessed the relationships among phytoplankton, DOM, and bacterial abundance in both field observations and laboratory experiments.

As a major production source of DOM, algal blooms release DOM into the environment, which supports bacterial growth. Few studies have studied the DOM dynamics in the water column of Keyport Harbor or the Raritan Bay area. Compared with nearby bays and estuaries, our measured DOC concentrations in the Keyport Harbor were close to

or higher than DOC in the Chesapeake Bay (138–249 µmol L^{-1}) (Rochelle-Newall and Fisher 2002), Long Island Sounds, NY (averaged 175 ± 16 µmol L^{-1}) (Vlahos and Whitney 2017), and Delaware Estuary (129–245 µmol L^{-1}) (Osterholz et al. 2016). The correlation heatmap in this study showed a significant positive correlation between chlorophyll-*a* and DOC (Fig. 8), suggesting algal production of DOC in Keyport Harbor. DOC concentrations were significantly higher in the bloom period, but DON concentrations were not (Fig. 5), indicating carbon-rich DOM in the bloom time. Phytoplankton extracellular release consists of up to 80% carbohydrate, predominantly in the form of polysaccharides (Myklestad 2000; Mühlenbruch et al. 2018), contributing to the observed carbon-rich DOM in the bloom time. Besides temporal change, DOC was also significantly different among sites, particularly between site 1 and site 4, between site 2 and site 4, and between site 3 and site 4 (Supplementary Table S2). Site 4 is close to a river mouth and had a significantly lower salinity than other sites (Table S1), suggesting that high DOC concentrations at site 4 might be attributed to terrigenous DOC input (Fig. 5a). Although an overall correlation between salinity and DOC at all sites was not significant (Fig. 8), significant differences observed for both salinity and DOC specifically between site 1 and 4 (Supplementary Table S2) indicate regional control of environmental conditions by river input. Coastal waters receive large fluxes of terrestrial organic matter through rivers, partly owing to human activities. This flux under anthropogenic perturbation has increased its lateral transport from rivers to estuaries compared with the pre-industrial level (Regnier et al. 2022; Martin and Bianchi 2024). DOC at site 3 in our data, in comparison with site 1 and site 2, was more similar to the DOC at site 4 (Fig. 5a). As site 3 is close to a historical landfill site, contact with landfill leachate likely increased the DOC concentration in the coastal water. DOM makes up more than 80% of the total organic matter in landfill leachate (He et al. 2006). Landfill leachate includes straight-chain organic acids, proteins, and humic substances in natural DOM and aromatic acids, terpenes, halogenated organics, indoles, and phenols in anthropogenic DOM, which can pollute groundwater nearby (Christensen et al. 1998; Huo et al. 2008; Zheng et al. 2024). However, more studies on specific compound biomarkers such as colored DOM (CDOM), amino acids, or carbon isotopic analysis are needed to identify the exact sources of DOC over spatiotemporal scales in the Keyport coastal water (Duan and Bianchi 2007; Lu et al. 2009; Cawley et al. 2012; Cheong et al. 2024).

Up to 50% of primary production released as DOM is used by bacteria in the sea via the microbial loop (Azam et al. 1983). The quality of DOM can be assessed through its utilization by bacteria. In this study, DOC varied not only in quantity between the bloom and nonbloom seasons but also in quality over the seasons. DOC supported higher bacterial abundance in the bloom time (Fig. 6) and positively correlated to bacterial abundance (Fig. 8), indicating more bioavailable DOC in the bloom time than in the nonbloom time. In general, a 10 °C increase in the average temperature from the nonbloom period to the bloom period as observed in this study would lead to a doubling of the rate of bacterial growth and twice as much bacterial abundance in the bloom time compared with the nonbloom time (Toolan 2001). An average threefold increase and up to four- to tenfold increase of bacterial abundance, substantially larger than doubling, in the bloom time relative to the nonbloom time (Fig. 6) indicates that, although bacterial abundance was positively correlated to temperature (Fig. 8), temperature was not the sole factor shaping the bacterial growth and DOC contributed substantially to bacterial biomass increase. While phytoplankton is the major source of DOC, other sources of DOC from zooplankton, viral lysis, and particle dissolution cannot be excluded from the environmental observations (Carlson et al. 2024). Microbial remineralization incubations in this study specifically investigated the interaction between bacteria and phytoplankton–DOM. Rapid phytoplankton lysate DOM degradation by bacteria and bacterial growth within a short incubation time in both experiments (Fig. 7) pointed to a strong bacterial response to phytoplankton–DOM. Phytoplankton lysate contains intracellular DOM components of phytoplankton cells, representing more concentrated labile substrates, in contrast to control, for bacteria after cell lysis such as during the algal bloom senescent stage in the natural environment. After phytoplankton lysate amendment, maximal bacterial abundance reached a similar level in bloom and nonbloom seasons, indicating that labile DOM was a limiting factor of bacterial production in the Keyport water and ambient bacteria responded opportunistically whenever it became available. The higher lability of ambient DOC to bacteria in the bloom time is further elaborated in the microbial remineralization experiments conducted at similar temperatures between two seasons. A higher removal percentage of ambient DOC (control treatment) and more bacteria growth were observed during the bloom period than the nonbloom period (Fig. 7), suggesting that DOC in the bloom time, of which a proportion was produced by phytoplankton, was more accessible to bacteria during the short incubation time and that DOC played an important role in shaping the bacterial dynamics apart from the temperature factor. Note that the majority ($>80\%$) of the DOC was not degraded by bacteria within 2 weeks, and this semilabile or refractory DOC is either transformed DOC from in situ production or allochthonous DOC. The salinity of the water collected for incubation experiments was not significantly different between the two seasons (25 ppt in August versus 26 ppt in November, Table S1), potentially owing to canceling effects from both terrigenous input and continental shelf ocean water exchange

in the nonbloom (November) season (Supplementary Fig. S4). Surface currents moved in the direction from Raritan Bay to New York/New Jersey Bight (Atlantic continental shelf) in August, while in the opposite direction in November, suggesting potential input from ocean water with different DOM quality in the nonbloom season. The types of bacteria degrading DOM of different quality are diverse, with specialists favored by terrigenous/ocean-water DOM or algal DOM only and generalists capable of degrading both types of DOM (Medeiros et al. 2017; Liu et al. 2020; Figueroa et al. 2021). Potentially different bacterial communities over seasons also affected DOC degradation patterns and total bacterial growth between two incubation experiments. Although these laboratory incubation experiments cannot exactly mimic the natural conditions, they isolated controlled variables and provided insights into the different responses of bacteria to environmental conditions across seasons.

In conclusion, this study combined analyses of nutrients, phytoplankton, DOM, and bacteria in the Keyport Harbor coastal water over both temporal and spatial scales to establish a water quality baseline coherent with the limited historical data in this underrepresented area. The collected datasets also fill the gap of the scarce information on DOM dynamics and phytoplankton–DOM–bacteria interactions in this region. Given the relationship between nitrogen nutrients and phytoplankton biomass, coastal management related to the control of land input of nitrogen is necessary. Switching from nitrogen-limited in the bloom time to phosphorus-limited water in the nonbloom time also calls for an adaptive management plan over seasons. The monitored nutrient values here also provide scientific evidence for setting up numerical nutrient criteria for the eutrophication mitigation strategy in the future. This study also facilitates more understanding of how eutrophication and algal blooms influence carbon cycling in the coastal water. Building upon this study, a long-term monitoring program including both chemical and biological parameters, such as nutrients, organic matter, and phytoplankton–bacteria interactions, in the Keyport coastal water is not just useful but crucial for promoting citizen awareness, supporting the comprehensive control and application of TMDL standards by the government, integrating land and sea management for coastal water quality, and assessing carbon cycling in the coastal regions, which serve an essential regulating role between land use input and export to offshore.

Declarations

References

Amin SA, Green DH, Hart MC, Küpper FC, Sunda WG, Carrano CJ (2009) Photolysis of iron–siderophore chelates promotes bacterial–algal mutualism. Proc Natl Acad Sci 106:17071–17076

Amin SA, Hmelo LR, van Tol HM, Durham BP, Carlson LT, Heal KR et al (2015) Interaction and signalling between a cosmopolitan phytoplankton and associated bacteria. Nature 522:98–101

Arandia-Gorostidi N, Krabberød AK, Logares R, Deutschmann IM, Scharek R, Morán XAG et al (2022) Novel interactions between phytoplankton and bacteria shape microbial seasonal dynamics in coastal ocean waters. Front Marine Sci 9:901201

Azam F, Fenchel T, Field JG, Gray JS, Meyerreil LA, Thingstad F (1983) The ecological role of water-column microbes in the sea. Mar Ecol-Prog Ser 10:257–263

Bagheri S (2017) New York/New Jersey nearshore waters—a case study in NY/NJ. Hyperspectral remote sensing of nearshore water quality: a case study in New York/New Jersey. Springer International Publishing, Cham, pp 19–27

Berner C, Bertos-Fortis M, Pinhassi J, Legrand C (2018) Response of microbial communities to changing climate conditions during summer cyanobacterial blooms in the Baltic Sea. Front Microbiol 9:1562

Bertrand EM, McCrow JP, Moustafa A, Zheng H, McQuaid JB, Delmont TO et al (2015) Phytoplankton-bacterial interactions mediate micronutrient colimitation at the coastal Antarctic sea ice edge. Proc Natl Acad Sci USA 112:9938–9943

Biddanda B, Benner R (1997) Carbon, nitrogen, and carbohydrate fluxes during the production of particulate and dissolved organic matter by marine phytoplankton. Limnol Oceanogr 42:506–518

Blanchet M, Pringault O, Panagiotopoulos C, Lefèvre D, Charrière B, Ghiglione J-F et al (2017) When riverine dissolved organic matter

(DOM) meets labile DOM in coastal waters: changes in bacterial community activity and composition. Aquat Sci 79:27–43

Bricker SB, Longstaff B, Dennison W, Jones A, Boicourt K, Wicks C, Woerner J (2008) Effects of nutrient enrichment in the nation's estuaries: a decade of change. Harmful Algae 8:21–32

Buchan A, LeCleir GR, Gulvik CA, Gonzalez JM (2014) Master recyclers: features and functions of bacteria associated with phytoplankton blooms. Nat Rev Microbiol 12:686–698

Camarena-Gómez MT, Ruiz-González C, Piiparinen J, Lipsewers T, Sobrino C, Logares R, Spilling K (2021) Bacterioplankton dynamics driven by interannual and spatial variation in diatom and dinoflagellate spring bloom communities in the Baltic Sea. Limnol Oceanogr 66:255–271

Carlson CA, Liu S, Stephens BM, English CJ (2024) DOM production, removal, and transformation processes in marine systems. In: Hansell DA, Carlson CA (eds) Biogeochemistry of marine dissolved organic matter, 3rd edn. Academic Press, Cham, pp 137–246

Cawley KM, Ding Y, Fourqurean J, Jaffé R (2012) Characterising the sources and fate of dissolved organic matter in Shark Bay, Australia: a preliminary study using optical properties and stable carbon isotopes. Mar Freshw Res 63:1098–1107

Cheong AYL, Annammala KV, Yong EL, Zhou Y, Nichols RS, Martin P (2024) Distribution of nutrients and dissolved organic matter in a eutrophic equatorial estuary: the Johor River and the East Johor Strait. Biogeosciences 21:2955–2971

Christensen JB, Jensen DL, GrØN C, Filip Z, Christensen TH (1998) Characterization of the dissolved organic carbon in landfill leachate-polluted groundwater. Water Res 32:125–135

Clark LB, Gobler CJ, Sañudo-Wilhelmy SA (2006) Spatial and temporal dynamics of dissolved trace metals, organic carbon, mineral nutrients, and phytoplankton in a coastal lagoon: Great South Bay, New York. Estuaries Coasts 29:841–854

CME Associates (2007) Natural resource inventory, Borough of Keyport, Monmouth county, New Jersey

Collos Y, Vaquer A, Bibent B, Souchu P, Slawyk G, Garcia N (2003) Response of coastal phytoplankton to ammonium and nitrate pulses: seasonal variations of nitrogen uptake and regeneration. Aquat Ecol 37:227–236

Crump BC, Bowen JL (2024) The microbial ecology of estuarine ecosystems. Ann Rev Mar Sci 16:335–360

Deck BL (1981) Nutrient-element distributions in the Hudson estuary: Columbia University

Dong M, Malsky B, Gamio L, Bloch M, Reinhard S, Abraham L et al (2023) Maps: tracking air quality and smoke from wildfires. The New York Times, p 3CfwH1B

Dorgham MM (2014) Effects of eutrophication. *Eutrophication: causes*. Consequences and Control: 2:29–44

Dortch Q (1990) The interaction between ammonium and nitrate uptake in phytoplankton. Marine Ecol Progress Series Oldendorf 61:183–201

Duan S, Bianchi TS (2007) Particulate and dissolved amino acids in the lower Mississippi and Pearl Rivers (USA). Mar Chem 107:214–229

EPA (2016) Surface water quality standards. NJSA 13: 10–1 et seq, 58: IOA-1 et seq, and 58: 1IA-I et seq

Figueroa D, Capo E, Lindh MV, Rowe OF, Paczkowska J, Pinhassi J, Andersson A (2021) Terrestrial dissolved organic matter inflow drives temporal dynamics of the bacterial community of a subarctic estuary (northern Baltic Sea). Environ Microbiol 23:4200–4213

Fox J, Weisberg S (2019) An R companion to applied regression. Sage, Thousand Oaks CA

Gastrich MD, Lathrop R, Haag S, Weinstein MP, Danko M, Caron DA, Schaffner R (2004) Assessment of brown tide blooms, caused by Aureococcus anophagefferens, and contributing factors in New Jersey coastal bays: 2000–2002. Harmful Algae 3:305–320

Gastrich, M.D. (2000) Harmful algal blooms in coastal waters of New Jersey. In New Jersey Department of Environmental Protection

Gobler CJ, Renaghan MJ, Buck NJ (2002) Impacts of nutrients and grazing mortality on the abundance of Aureococcus anophagefferens during a New York brown tide bloom. Limnol Oceanogr 47:129–141

Gomez Isaza DF, Cramp RL, Franklin CE (2022) Fire and rain: a systematic review of the impacts of wildfire and associated runoff on aquatic fauna. Glob Change Biol 28:2578–2595

Grossart HP, Czub G, Simon M (2006) Algae-bacteria interactions and their effects on aggregation and organic matter flux in the sea. Environ Microbiol 8:1074–1084

Halewood E, Opalk K, Custals L, Carey M, Hansell DA, Carlson CA (2022) Determination of dissolved organic carbon and total dissolved nitrogen in seawater using high temperature combustion analysis. Front Mar Sci 9:1061646

Hansell DA (2013) Recalcitrant dissolved organic carbon fractions. Ann Rev Mar Sci 5:421–445

Harding LW, Gallegos CL, Perry ES, Miller WD, Adolf JE, Mallonee ME, Paerl HW (2016) Long-term trends of nutrients and phytoplankton in Chesapeake Bay. Estuaries Coasts 39:664–681

Harrell Jr. F, Dupont C (2019) Hmisc: Harrell Miscellaneous

He P-J, Xue J-F, Shao L-M, Li G-J, Lee D-J (2006) Dissolved organic matter (DOM) in recycled leachate of bioreactor landfill. Water Res 40:1465–1473

He Y, Zhang P, Xu F, Zhao L, Zhang J (2023) Seasonal nutrients variation, eutrophication pattern, and chlorophyll a response adjacent to Guangdong coastal water, China. Front Marine Sci 10:1236609

Heck KL, Valentine JF (2007) The primacy of top-down effects in shallow benthic ecosystems. Estuaries Coasts 30:371–381

Holmes RM, Aminot A, Kérouel R, Hooker BA, Peterson BJ (1999) A simple and precise method for measuring ammonium in marine and freshwater ecosystems. Can J Fish Aquat Sci 56:1801–1808

Huo S, Xi B, Yu H, He L, Fan S, Liu H (2008) Characteristics of dissolved organic matter (DOM) in leachate with different landfill ages. J Environ Sci 20:492–498

Jeffries HP (1962) Environmental characteristics of Raritan Bay, a polluted estuary. Limnol Oceanogr 7:21–31

Jones MN (1984) Nitrate reduction by shaking with Cadmium—alternative to Cadmium columns. Water Res 18:643–646

Kassambara, A. (2023) ggpubr: 'ggplot2' based publication ready plots.

Kennish MJ (2009) Eutrophication of mid-Atlantic coastal bays. Bull New Jersey Acad Sci 54:1–8

Kennish MJ, Bricker SB, Dennison WC, Glibert PM, Livingston RJ, Moore KA et al (2007) Barnegat Bay-Little Egg Harbor estuary: case study of a highly eutrophic coastal bay system. Ecol Appl 17:S3–S16

Kennish MJ, Fertig BM, Lathrop RG (2012) Assessment of nutrient loading and eutrophication in Barnegat Bay-Little Egg Harbor, New Jersey in support of nutrient management planning

Kleinfelder (2013) Phase II raritan river basin nutrient TMDL study watershed model and TMDL calculations

Liu S, Baetge N, Comstock J, Opalk K, Parsons R, Halewood E et al (2020) Stable isotope probing identifies bacterioplankton lineages capable of utilizing dissolved organic matter across a range of bioavailability. Front Microbiol 11:580397

Lomas MW, Glibert PM (2000) Comparisons of nitrate uptake, storage, and reduction in marine diatoms and flagellates. J Phycol 36:903–913

Lorenzen CJ (1967) Determination of chlorophyll and pheo-pigments: spectrophotometric equations. Limnol Oceanogr 12:343–346

Lu F, Chang C-H, Lee D-J, He P-J, Shao L-M, Su A (2009) Dissolved organic matter with multi-peak fluorophores in landfill leachate. Chemosphere 74:575–582

Maest AS, Crerar DA, Stallard RF, Ryan JN (1990) Metal and nutrient behavior in the Raritan estuary, New Jersey, U.S.A.: the effect of multiple freshwater and industrial waste inputs. Chem Geol 81:133–149

Martin P, Bianchi TS (2024) Organic carbon cycling and transformation. In: Baird D, Elliott M (eds) Treatise on estuarine and coastal science (Second Edition). Academic Press, Oxford, pp 164–224

Maurer D, Watling L, Bottom D, Pembroke A (1978) Seasonal fluctuation of water quality (nutrients and pigments) in lower Delaware Bay. Hydrobiologia 60:203–211

McCarthy, A.J. (1965) An ecological study of the phytoplankton of Raritan Bay. In: ETD Collection for Fordham University

Medeiros PM, Seidel M, Gifford SM, Ballantyne F, Dittmar T, Whitman WB, Moran MA (2017) Microbially-mediated transformations of estuarine dissolved organic matter. Front Mar Sci 4:49

Miller CB (2004) Biological oceanography. Blackwell Publishing, Hoboken

Minor EC, Simjouw J-P, Mulholland MR (2006) Seasonal variations in dissolved organic carbon concentrations and characteristics in a shallow coastal bay. Mar Chem 101:166–179

Mühlenbruch M, Grossart HP, Eigemann F, Voss M (2018) Minireview: phytoplankton-derived polysaccharides in the marine environment and their interactions with heterotrophic bacteria. Environ Microbiol 20:2671–2685

Myklestad SM (2000) Dissolved organic carbon from phytoplankton. In: Wangersky PJ (ed) Marine chemistry. Springer Berlin Heidelberg, Berlin, Heidelberg, pp 111–148

Nelson DM, Tréguer P, Brzezinski MA, Leynaert A, Quéguiner B (1995) Production and dissolution of biogenic silica in the ocean: revised global estimates, comparison with regional data and relationship to biogenic sedimentation. Global Biogeochem Cycles 9:359–372

Nielsen TG, Kiørboe T (1991) Effects of a storm event on the structure of the pelagic food web with special emphasis on planktonic ciliates. J Plankton Res 13:35–51

NJDEP (2016) Review of total maximum daily loads (TMDLs) for the non-tidal Raritan River basin: Addressing total phosphorus, dissolved oxygen, pH and total suspended solids New Jersey.

NJDEP (2022). Overburdened communities. https://njdep.maps.arcgis.com/apps/webappviewer/index.html?id=34e507ead25b4aa5a5051dbb85e55055. Accessed 10 Oct 2024

O'Dell K, Hornbrook RS, Permar W, Levin EJT, Garofalo LA, Apel EC et al (2020) Hazardous air pollutants in fresh and aged western US wildfire smoke and implications for long-term exposure. Environ Sci Technol 54:11838–11847

Osterholz H, Kirchman DL, Niggemann J, Dittmar T (2016) Environmental drivers of dissolved organic matter molecular composition in the Delaware Estuary. Front Earth Sci 4:95

Paudel B, Weston N, O'Connor J, Sutter L, Velinsky D (2017) Phosphorus dynamics in the water column and sediments of Barnegat Bay, New Jersey. J Coastal Res 78:60–69

Paul MJ, LeDuc SD, Lassiter MG, Moorhead LC, Noyes PD, Leibowitz SG (2022) Wildfire induces changes in receiving waters: a review with considerations for water quality management. Water Resour Res 58:e2021WR030699

Pinhassi J, Sala MM, Havskum H, Peters F, Guadayol O, Malits A, Marrasé C (2004) Changes in bacterioplankton composition under different phytoplankton regimens. Appl Environ Microbiol 70:6753–6766

Porter KG, Feig YS (1980) The use of DAPI for identifying and counting aquatic microflora. Limnol Oceanogr 25:943–948

Regnier P, Resplandy L, Najjar RG, Ciais P (2022) The land-to-ocean loops of the global carbon cycle. Nature 603:401–410

Ren, L. (2013) Baseline characterization of phytoplanton and harmful algal blooms in Barnegat Bay-Little Egg Harbor, New Jersey. In

New Jersey department of environmental protection, division of science, research and environmental health. Trenton, NJ, pp. 1–72

Riley GA (1941) Plankton studies. IV Georges Bank. Bull Bingham Oceanogr Coll 7(4):1–73

Riley, G.A., Conover, S.A., Deevey, G.B., Conover, R.J., Wheatland, S.B., Harris, E., and Sanders, H.L. (1956) Volume 15. Article 1. Oceanography of long Island sound, 1952–1954. Bull Bingham Oceanogr Coll

Rochelle-Newall EJ, Fisher TR (2002) Chromophoric dissolved organic matter and dissolved organic carbon in Chesapeake Bay. Mar Chem 77:23–41

Rothenberger MB, Swaffield T, Calomeni AJ, Cabrey CD (2014) Multivariate analysis of water quality and plankton assemblages in an urban estuary. Estuaries Coasts 37:695–711

Rothenberger M, Gleich SJ, Flint E (2023) The underappreciated role of biotic factors in controlling the bloom ecology of potentially harmful microalgae in the Hudson-Raritan Bay. Harmful Algae 124:102411

Ryther JH, Dunstan WM (1971) Nitrogen, phosphorus, and eutrophication in the coastal marine environment. Science 171:1008–1013

Schlitzer, R. (2022) Ocean data view version 5.6.2. https://odv.awi.de/. Accessed 04 Apr 2022

Smayda TJ, Borkman DG (2008) Nutrient and plankton dynamics in Narragansett Bay. In: Desbonnet A, Costa-Pierce BA (eds) Science for ecosystem-based management: Narragansett Bay in the 21st century. Springer New York, New York, NY, pp 431–484

Smith DC, Steward GF, Long RA, Azam F (1995) Bacterial mediation of carbon fluxes during a diatom bloom in a mesocosm. Deep Sea Res Part II 42:75–97

Stephens BM, Opalk K, Petras D, Liu S, Comstock J, Aluwihare LI et al (2020) Organic matter composition at Ocean Station Papa affects its bioavailability, bacterioplankton growth efficiency and the responding taxa. Front Mar Sci 7:590273

Strickland JDH, Parsons TR (1968) A practical handbook of seawater analysis. Queen's Printer, Ottawa

Sylvan JB, Ammerman JW (2013) Seasonal distributions of organic nutrients on the Louisiana continental shelf and their implications for nutrient limitation and hypoxia formation. Mar Chem 154:113–123

Teeling H, Fuchs BM, Bennke CM, Krüger K, Chafee M, Kappelmann L et al (2016) Recurring patterns in bacterioplankton dynamics during coastal spring algae blooms. eLife 5:e11888

Toolan T (2001) Coulometric carbon# based respiration rates and estimates of bacterioplankton growth efficiencies in Massachusetts Bay. Limnol Oceanogr 46:1298–1308

Vlahos P, Whitney MM (2017) Organic carbon patterns and budgets in the Long Island Sound estuary. Limnol Oceanogr 62:S46–S57

Wang S, Zhou F, Chen F, Zhu Q, Meng Y (2024) Spatial and seasonal variations of chlorophyll a in Zhanjiang Bay, China, and controlling factors. Front Mar Sci 11:1329864

Wickham H (2007) Reshaping data with the reshape package. J Stat Softw 21:1–20

Wickham H (2016) ggplot2: elegant graphics for data analysis

Xiao X, Powers LC, Liu J, Gonsior M, Zhang R, Zhang L et al (2022) Biodegradation of terrigenous organic matter in a stratified large-volume water column: implications of the removal of terrigenous organic matter in the coastal ocean. Environ Sci Technol 56:5234–5246

Zheng J, Wang X-G, Sun Y, Wang Y-X, Sha H-Q, He X-S, Sun X-J (2024) Natural and anthropogenic dissolved organic matter in landfill leachate: composition, transformation, and their coexistence characteristics. J Hazard Mater 465:133081

Springer